Journal Pre-proof

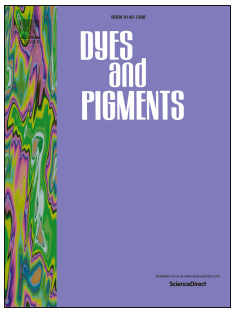

Temperature- and solvent-induced solid-state emission and AIEE property of a pyrene-based sulfide compound

Hao Sun, Jian-Hua Wei, Li-Hua Xu, Yan Jiang, Bao-Xi Miao, Zhong-Hai Ni

PII: S0143-7208(19)32912-2

DOI: https://doi.org/10.1016/j.dyepig.2020.108299

Reference: DYPI 108299

To appear in: *Dyes and Pigments*

Received Date: 12 December 2019

Revised Date: 19 February 2020

Accepted Date: 19 February 2020

Please cite this article as: Sun H, Wei J-H, Xu L-H, Jiang Y, Miao B-X, Ni Z-H, Temperature- and solvent-induced solid-state emission and AIEE property of a pyrene-based sulfide compound, *Dyes and Pigments* (2020), doi: https://doi.org/10.1016/j.dyepig.2020.108299.

This is a PDF file of an article that has undergone enhancements after acceptance, such as the addition of a cover page and metadata, and formatting for readability, but it is not yet the definitive version of record. This version will undergo additional copyediting, typesetting and review before it is published in its final form, but we are providing this version to give early visibility of the article. Please note that, during the production process, errors may be discovered which could affect the content, and all legal disclaimers that apply to the journal pertain.

© 2020 Published by Elsevier Ltd.

Hao Sun: Investigation, Writing - original draft.

Jian-Hua Wei: Investigation, Validation, Visualization, Software.

Li-Hua Xu: Investigation, Validation, Visualization.

Yan Jiang: Investigation, Validation, Visualization.

Bao-Xi Miao: Investigation, Validation, Visualization.

Zhong-Hai Ni: Writing - review & editing, Supervision, Project administration.

Journal Pre-proof

Graphic Abstract

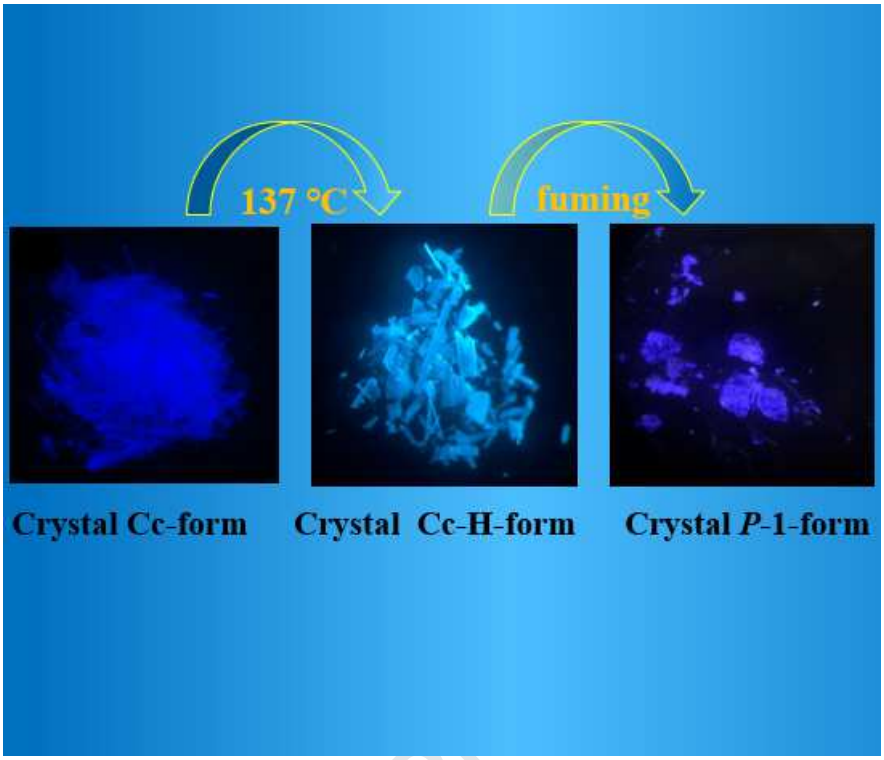

Journal Pre-proof

Journal Pre-proof

Temperature- and solvent-induced solid-state emission and AIEE property of a pyrene-based sulfide compound

Hao Sun, Jian-Hua Wei, Li-Hua Xu, Yan Jiang, Bao-Xi Miao, Zhong-Hai Ni*

School of Chemical Engineering and Technology, China University of Mining and Technology, Xuzhou, 221116, People's Republic of China;

Corresponding author E-mail: nizhonghai@cumt.edu.cn (Z. H. Ni)

Abstract

A new organic compound **PyStBu** was designed and synthesized, which exhibits successive solid-state emission changes induced by heating and DCM vapors fuming. Intermolecular interaction changes or heat-induced crystal surface layer changes may be reasonable for the emission change of Cc-form after heating. In addition, crystal packing changes may be the dominant reason for different photophysical properties of Cc-H-form and P-1-form after DCM fuming. These observations provide reference for tuning property of organic solid-state luminescence materials and designing smart crystal luminescent materials. In addition, **PyStBu** exhibits aggregation-induced emission enhancement (AIEE) property with interesting "on–off–on" optical switching behavior.

Keywords: single crystal-to-single crystal (SCSC) structural transformation, aggregation-induced emission enhancement (AIEE), pyrene, sulfide, crystal packing

1 Introduction

Organic solid-state luminescence materials especially those with tunable luminescence properties have attracted extensive attention due to their wide application in various fields.[1-6] Generally, alteration of the style of solid-state molecular packing is considered as a promising

Journal Pre-proof

method for turning luminescence properties of organic solid molecules because of the strong dependence of their solid-state fluorescence on molecular structure and intermolecular interactions.[7-11] Considering the difficulty and time-consuming synthesis of materials, an approach based on application of physical stimuli (such as, light, temperature, and pressure) to tune emission properties of organic solids exhibits many advantages such as easier operation, simple equipment, efficient conversion and so on.[12,13] Single-crystal-to-single-crystal (SCSC) phase transition provides a good chance to investigate structure-property relationships of functional materials because the original crystals will maintain their single crystallinity after the SCSC transformation and the changed structures can be accurately characterized using single-crystal X-ray diffraction.[14,15] Up to date, the reports on SCSC transformation are mainly focused on metal complexes and metal–organic frameworks (MOFs) and the relevant studies are very fruitful.[14-16] However, although many studies on the modulation of organic solid-state optical properties have been reported, molecular-level understanding of the relationship between structure and resulting luminescence property is deficient owing to the difficulty of obtaining accurate structural information accounting for the transition of luminescence properties.[17-23] Therefore, investigation on organic SCSC is a meaningful work and will be helpful for understanding the structure-property relationships of organic solid-state luminescence materials and developing organic crystal materials.

Herein, we report the design and synthesis of a new organic pyrene-based sulphide compound ((4-(*tert*-butyl)phenyl)(7-(*tert*-butyl)pyren-1-yl)sulfane (**PyStBu**) (Scheme 1) which exhibits successive solid-state emission changes induced by heating and organic

Journal Pre-proof

solvents vapours fuming. Significant changes of emission wavelength and crystal colours are observed. These observations provide a chance to deeply understand the relationship between optical properties and structure on molecular level. In addition, **PyStBu** exhibits aggregation-induced emission enhancement property with interesting "on–off–on" optical switching behaviour.

2 Experimental section

2.1 Synthesis

2.2.1 Synthesis of 2-(*tert*-butyl)pyrene (1)

Firstly, 20 g (100 mmol) pyrene was dissolved in 200 mL CS_2. The above solution was heated to 40 °C under the protection of nitrogen. 22 g (161 mmol) $AlCl_3$ was quickly added into the above solution that was stirred for 10 min. Secondly, 15 g (161 mmol) t-butyl chloride was dissolved in 100 mL CS_2, and the solution was added into the above mixture. The mixture was refluxed for 5 h. The reaction mixture was cooled down to room temperature and poured into ice water after the reaction was completed. The mixture was diluted with hydrochloric acid to adjust the pH to 4. Then, the above mixture was extracted with DCM, washed with water, dried over $MgSO_4$, filtered and concentrated. The concentrated product was purified by silica gel flash column chromatography using hexane as the eluent. Yield: 24 g, 92%. ^{1}H NMR (300 MHz, $CDCl_3$): δ = 1.59 (s, 9H), 8.18 (d, J = 9.2 Hz, 2H), 8.30 (s, 2H), 8.37 (d, J = 9.2 Hz, 2H), 8.47 (s, 1H). ^{1}H NMR spectrum of **1** completely agreed with reported values.[24]

2.2.2 Synthesis of 1-bromo-7-(*tert*-butyl)pyrene (2)

1 g (4 mmol) **1** was dissolved in 20 mL DCM, the above solution was stirred at -78 °C for 10 min. Then 0.64 g Br_2 was dissolved in 10 mL DCM, which was slowly added into the above solution. Then the above mixture was stirred for 10h at room temperature. The reaction mixture was poured into $NaHSO_3$ solution after the reaction is completed. The under organic phase was dried over $MgSO_4$, filtered, and concentrated. The concentrated product was purified by silica gel flash column chromatography using hexane as the eluent. Yield: 0.97 g, 72%. ^{1}H NMR (300 MHz, $CDCl_3$): δ = 8.41 (d, J = 9 Hz, 1H), 8.27 (d, J = 3 Hz, 2H), 8.14–8.20 (m, 2H), 8.08 (d, J = 9 Hz, 1H), 7.96–8.01 (m, 2H), 1.60 (s, 9H). ^{1}H NMR spectrum of **2** completely agreed with reported values.[24]

2.2.3 Synthesis of (4-(*tert*-butyl)phenyl)(7-(*tert*-butyl)pyren-1-yl)sulfane (PyStBu)

0.58 g (3.5 mmol) 4-*tert*-Butylthiophenol, 1 g (3 mmol) **2** and 20 mL DMF was added to a 100 ml round bottom flask. The above mixture was stirred for 10 min in an ice bath under the protection of N_2. Then, 0.134 g (3.5 mmol) NaH (60%) was slowly added to the above flask in batches and the mixture was stirred for another 10 min. After all the generated hydrogen by the reaction was discharged, the mixture was refluxed for 10 h, poured into water, extracted with DCM and washed with water for three times. The organic phase was dried over $MgSO_4$, filtered, and concentrated. The concentrated product was purified by silica gel flash column chromatography using hexane as the eluent. Yield: 1.1 g, 84%. ^{1}H NMR (600 MHz, $CDCl_3$) δ 8.67 (d, J = 9.2 Hz, 1H), 8.28 (s, 2H), 8.18 – 8.08 (m, 4H), 8.05 (d, J = 8.9 Hz, 1H), 7.29 – 7.27 (m, 2H), 7.19 – 7.14 (m, 2H), 1.62 (s, 9H), 1.29 (s, 9H). ^{13}C NMR (150 MHz, $CDCl_3$), δ(TMS, ppm): 149.48, 149.29, 133.96, 131.95, 131.61, 131.23, 131.11, 130.85, 128.78, 128.60, 128.50, 128.19, 127.11, 126.17, 125.27, 124.99, 124.79, 122.82, 122.81, 122.69, 35.27, 34.45, 31.92, 31.27. MALDI-TOF MS (m/z): calcd for $C_{30}H_{30}S$ 422.2068, found 422.2073.

Journal Pre-proof

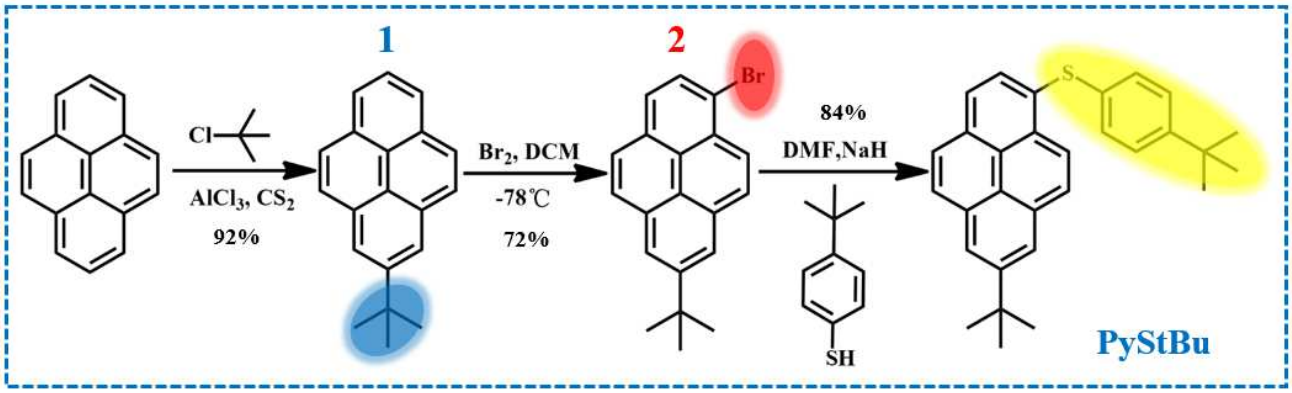

Scheme 1 Synthetic routes of compound **PyStBu**.

3 Results and discussions

3.1 Temperature-induced emission change

By slow evaporating of mixture solution of dichloromethane (DCM) and hexane (Hex), needle-like crystal of **PyStBu** with Ccc2 space group (named as Cc-form, CCDC 1964639) was obtained. The crystal structure of Cc-form is shown in Figure 1A and the crystal data is illustrated in Table S1. Cc-form crystal exhibits intense deep-blue emission with a maximum emission peak at about 420 nm (Φ_F=0.1132) (Figure 2B). Interestingly, the initial blue emission of Cc- form gradually turns into blue-green emission when it is heated from 25 °C to 137 °C (Figure 2D). The initial emission peak at about 420 nm red-shifts to 460 nm. The crystal will melt into liquid when the heated temperature reaches to its melting point at about 141 □. In order get insight into the solid-state fluorescence change properties of Cc-form, the powder XRD and differential scanning calorimetry (DSC) analysis were performed to study the phase characteristics of Cc-form. DSC analysis of Cc-form reveals that it exhibits an exothermic peak at approximately 137 °C indicating that Cc-form crystal could undergo a

phase transformation (Figure S1). Fortunately, the crystal structure of Cc-H-form (Heating Cc-form at 137 °C for 5 minutes and then colling down to room temperature to produce Cc-H- form (Φ_F=0.5968), Cc-H form is in fact an annealed Cc form. CCDC 1964640) can be characterized by single-crystal X-ray diffraction. The results of XRD analysis of Cc-form and Cc-H-form consistent with the simulated pattern generated by the single crystal structure (Figure 2C). The different peak patterns of Cc-form and Cc-H-form indicate that the structural transformation from Cc-form to Cc-H-form occurred. Moreover, the difference in fluorescence lifetime of Cc-form and Cc-H-form indicates changes of crystal microenvironment (Figure S2).[25]

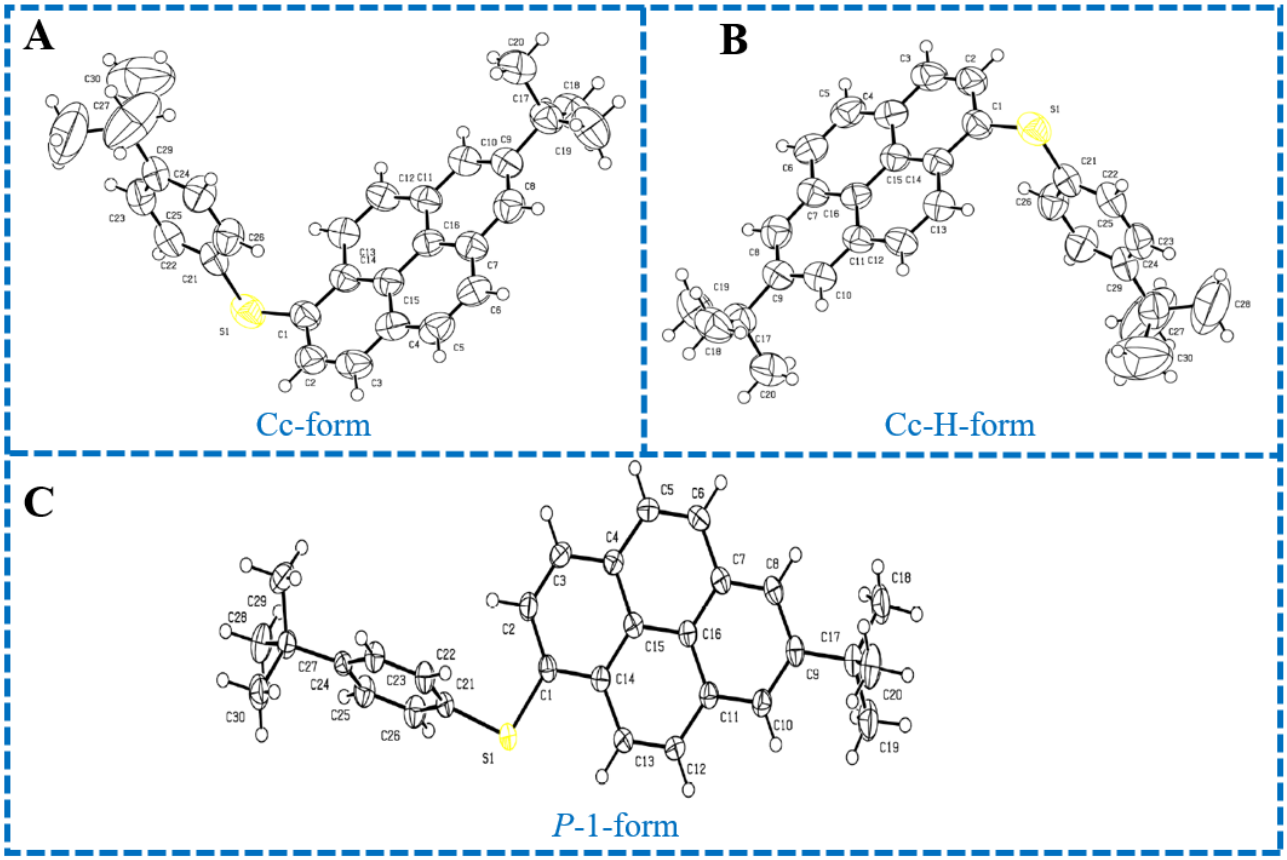

Figure 1 The crystal structure of Cc-form (A), Cc-H-form (B) and *P*-1-form (C).

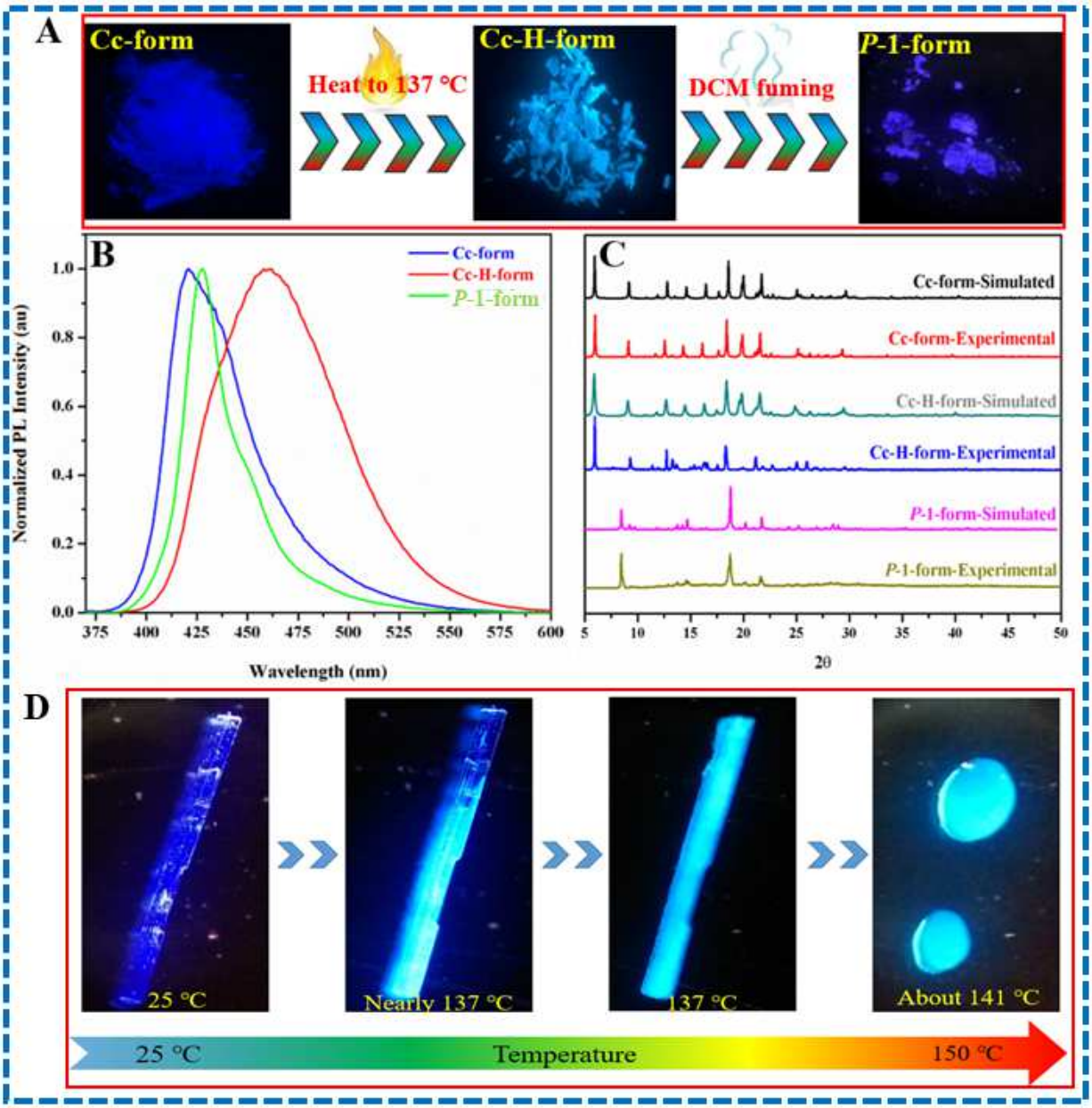

Figure 2 (A) Images of Cc-form, Cc-H-form and *P*-1-form under 365 UV in the process of SCSC structural transformation. (B) Normalized PL spectra of Cc-form, Cc-H-form and *P*-1-form. (C) The simulated and experimental XRD data of Cc-form, Cc-H-form and *P*-1-form. (D) The images of Cc-form in the heating process. For PL measurement, excitation wavelength: 365 nm. Images are taken under 365 nm UV light.

In order to understand the SCSC phase transformation and luminescence change in depth, the crystal structure analysis was performed. The crystal data of Cc-H-form is given in Table S1 and its crystal structure are shown in Figure 1B. The packing arrangement of Cc-form and Cc-H-form are shown in Figure 3. As is shown, Cc-form crystalizes in the orthorhombic system with Ccc2 space group. One Cc-form molecule and adjacent molecule are held together by weak C–H···π and weak π···π interactions to form 1D chains and then further connected by hydrogen bond interaction to form 3D supramolecular network. Structure determination indicates that Cc-H-form has the same Ccc2 space group with Cc-form. However, the cell volume decreases from 4702.1 (5) to 4567 (6) $Å^3$, indicating a contraction of crystal Cc-H-form.[26] Such changes may lead to crack of crystal. As can be seen from the SEM images of Cc-form and Cc-H-form, the surface of Cc-form is smooth without cracks (Figure 4A and Figure 4B), however, obvious cracks can be seen on the rough surface of Cc-H-form (Figure 4C and Figure 4D). Notably, the distances of the same kinds of C–H···π and π···π interaction in Cc-H-form become shorter than that in Cc-form (① and ② marked in Figure 3B and Figure 3D). The shorter interaction distance indicates stronger π···π interaction that may be reasonable for the red shift of emission of Cc-H-form. However, the π···π interaction in Cc-H-form is still weak due to relative large dihedral angle between the interactional molecules. Moreover, there is only three kinds of weak interactions (one kind of H…H contact, one kind of C–H···π interaction and one π···π interaction) in Cc-form. On the contrary, six kinds of weak interactions (one H…H contact, four kinds of C–H···π interaction and one π···π interaction) are observed in the Cc-H-form crystal (The detailed data of the interactions is shown in Table S2). The distance of these C–H···π interactions in Cc-H-form

are also shorter than that of Cc-form, which indicates stronger intermolecular interaction between adjacent molecule in Cc-H-form. Such more multiple and stronger interactions in Cc-H-form will inhibit internal rotations and vibration, which may be reasonable for the stronger emission intensity and longer lifetime of Cc-H-form than Cc-form.[13,25,27-29] The excitation spectrum of Cc-form, Cc-H-form and P-1-form were measured and shown in Figure S3. As illustrated, the excitation spectrum of Cc-H-form exhibits broader and red-shifted features without fine vibrational structures compared to that of Cc-form and P-1-form, indicating the possible formation of ground state dimer. The broader emission spectra profile, red-shifted emission wavelength and longer fluorescence lifetime can also provide some information for the formation of dimer.

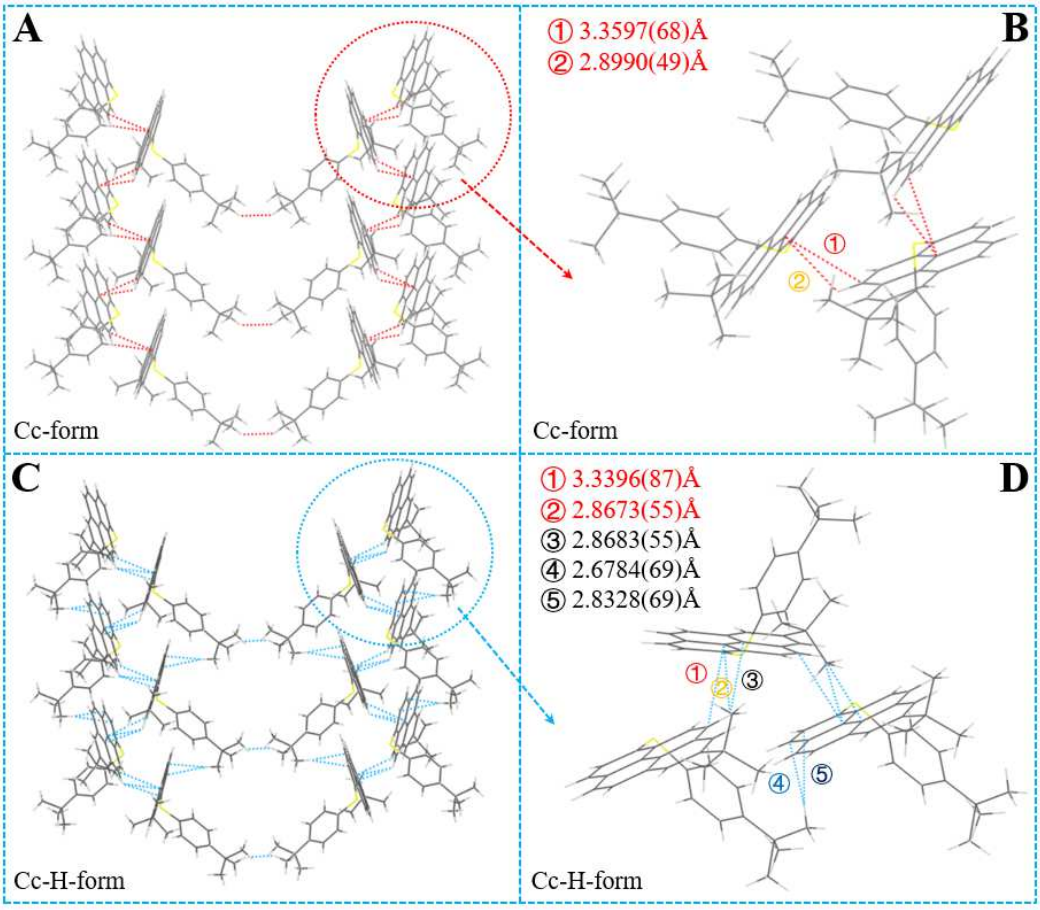

Figure 3 The crystal packing and intermolecular interaction of Cc-form ((A) and (B)) and

Cc-H-form ((C) and (D)).

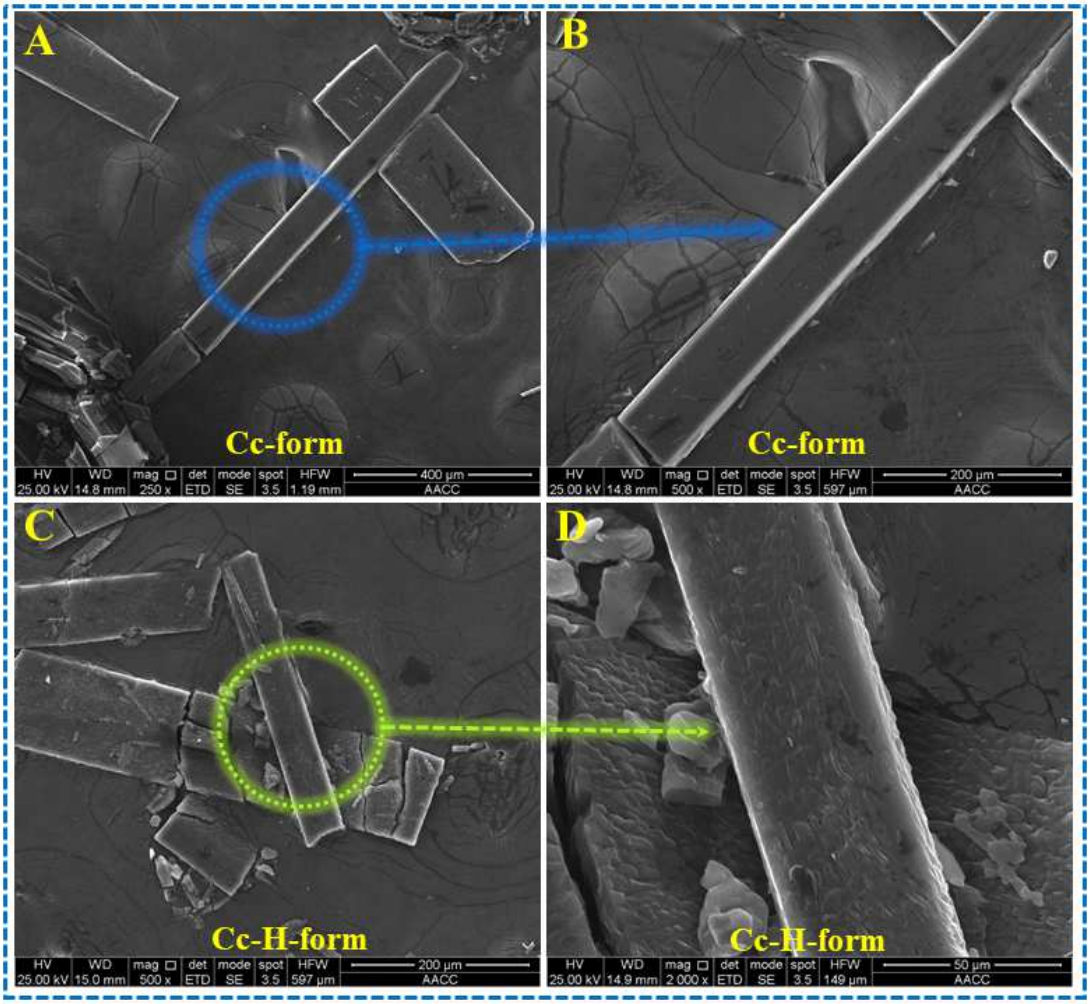

Figure 4 The SEM of Cc-form and Cc-H-form at different magnification times (A) Scale bar = 400 μm, (B) Scale bar = 200 μm, (C) Scale bar = 200 μm and (D) Scale bar = 50 μm.

Considering the phase transition peak of Cc-form is close to its melting point, another possible reason (changes of the crystal surface layer) for the emission change should be verified. The PL spectra of melted Cc-form (heated to the melted state and cooled down to room temperature) were shown in Figure S4. As illustrated, the emission peak of melted Cc-form is located at about 474 nm, which red shifts 14 nm compared with that of Cc-H-form. Moreover, the emission intensity also decreased obviously. The difference both

in emission wavelength and emission intensity indicates the different states of Cc-H-form and melted Cc-form. In addition, the diffraction images of Cc-form and Cc-H-form were provided in Figure S5. As illustrated, the bright and clear diffraction spots indicate that Cc-H-form keeps a good crystal state. The different emission properties of Cc-H-form and melted Cc-form also indicate that Cc-H-form is not in an obvious melted state. However, it would not be ruled out the possibility that the fluorescence behaviour of Cc-H-form is caused by the heat-induced crystal surface layer changes such as partial rupture and slight melt.

3.2 DCM vapors-induced emission change

Interestingly, Cc-H-form crystal also exhibits SCSC phase transition property. When Cc-H-form is exposed to DCM vapours for about 6 hours, Cc-H-form changes into flakes accompanied by emission colour change from blue-green emission to blue emission (named as *P*-1-form (Φ_F=0.1636), CCDC 1964641). The maximum emission wavelength of *P*-1-form locates at about 430 nm which is blue-shifted 30 nm compare with that of Cc-H-form. The different XRD results of Cc-H-form and *P*-1-form indicates the structural transformation (Figure 2C). Crystal structure analysis indicates that *P*-1-form crystalizes in the triclinic system with *P*-1 space group that is very different from Cc-form and Cc-H-form. In addition, the crystal packing model and weak interactions are different from that of Cc-form and Cc-H-form. The packing arrangement of *P*-1-form is shown in Figure 5. As is shown, along both the vertical and lateral directions, one *P*-1-form molecule interacts with six adjacent molecules through multiple weak interactions. Five kinds of weak interactions (one kind of C-H$\cdots$S interaction, three kinds of C-H$\cdots\pi$ interaction and one $\pi\cdots\pi$ interaction) are observed in *P*-1-form, which holds the molecule pairs together to form a 3D structure. The detailed

distance of them is shown in Table S2. The more intermolecular interaction especially C-H$\cdot\cdot\pi$ interaction than that of Cc-form indicating a more rigid framework of *P*-1-form. Different from the herringbone packing of Cc-form and Cc-H-form, *P*-1-form adopts a staggered parallel stacking. In crystal structure of *P*-1-form, two pyrene planes are parallel to each other with large slip (almost no overlap) and 3.245 Å interplanar distances forming staggered parallel stacking, which indicates a very weak $\pi\cdot\cdot\pi$ interactions between adjacent molecules. This may account for the blue-shifted emission of *P*-1-form compared with Cc-H-form. Besides, considering the different molecular conformation of Cc-form, Cc-H-form and *P*-1-form may influence their emission properties, we calculated the frontier molecular orbital of the three crystals with different conformations using density functional theory (DFT) based on the Gaussian 09 package. The highest occupied molecular orbitals (HOMOs) and the lowest unoccupied molecular orbitals (LUMOs) of Cc-form, Cc-H-form and *P*-1-form are very similar (Figure 6). The energy band gap variations and the energy changes induced by the different conformation are about 0.0003-0.0449 eV and 2×10^{-8}-0.0002 eV (Table 1). These results indicate that the influence of molecular conformational alteration on their emission properties is negligible and the crystal packing dominates the photo-physical properties of the crystals.[13,25,30]

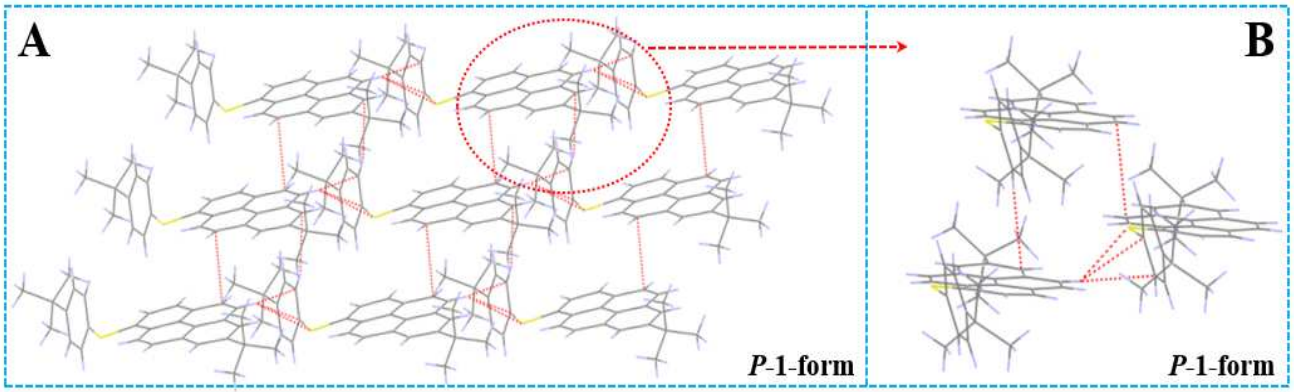

Figure 5 The crystal packing and intermolecular interactions of *P*-1-form.

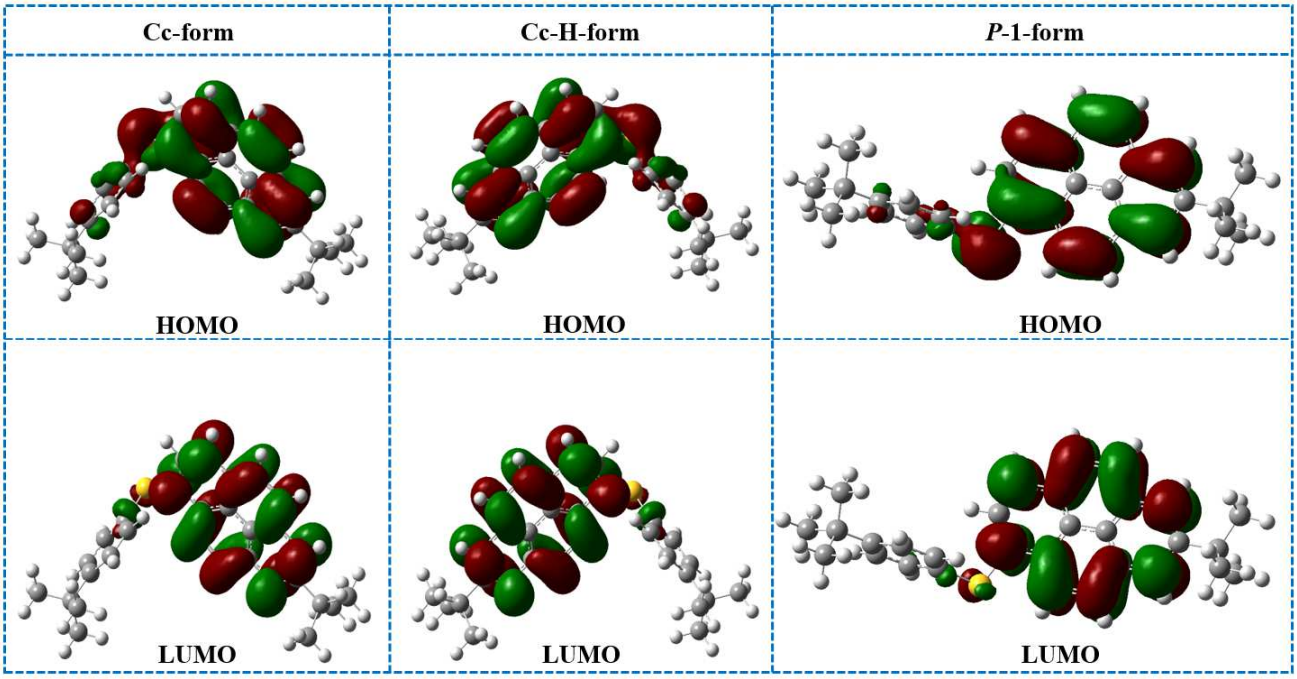

Figure 6 Calculated spatial distributions of HOMO and LUMO levels of crystal Cc-form, Cc-H-form and *P*-1-form based on B3LYP/6-31G* basis set.

.

Table 1 Calculated energy level of crystal Cc-form, Cc-H-form and *P*-1-form based on B3LYP/6-31G* basis set.

	Energy/a. u.	HOMO/eV	LUMO/eV	E/eV
Cc-form	-1559.22059564	-0.19731	-0.06105	-3.70818
Cc-H-form	-1559.22059566	-0.19731	-0.06104	-3.70791
***P*-1-form**	-1559.22084437	-0.18888	-0.05426	-3.66328

3.3 Aggregation-induced emission enhancement property (AIEE)

PyStBu is likely to exhibit AIEE property due to the introduction tert-butyl and rotable benzene ring around the pyrene core. The large steric hindrance of rotational benzene ring and tert-butyl can suppress the aggregation-caused quenching effect of PyStBu in aggregation state of solid state. **PyStBu** exhibits a good solubility in THF, however, it is almost insoluble in water. As illustrated in

Journal Pre-proof

Figure 7, **PyStBu** emits blue fluorescence in pure THF solution with an emission peak located at 399 nm is observed. Overall, with increase of water content in THF, the emission intensity gradually declines (water content from 0% to 70%). The fluorescence emission of **PyStBu** is almost quenched when the water content reached 70%. With further adding water into THF solution of **PyStBu**, the fluorescence intensity of the solution is starting to increase (water fraction, 80%) and a new emission peak at 480 nm is observed. As the moisture content increased further, the emission of **PyStBu** increased dramatically until the measured 95% water content. Throughout the entire process, an interesting "on–off–on" optical switching property is observed, the emission changes from deep-blue to light-blue to blue-green with the increase of water content (Figure 7B**)**. The above changes of emission tendency indicate that **PyStBu** maintains original efficient emission in dilute solution just like features of traditional dyes and exhibits typical AIEE property in aggregated state at the same time. In order to understand the nature of different light-emitting species, time-correlated single-photon counting (TCSPC) measurements were performed (Figure 8). As illustrated, the decay curve of **PyStBu** in pure THF solution is in good agreement with the two-order exponential decay curves (Figure 8A). In pure THF solution, a long-lived component with a lifetime (τ) of 3.24 ns (4.4%) and a short-lived species with lifetime of 0.59 ns (95.6%) for emission monitored at 400 nm were observed. According to previous reports, the above shorter and longer decay values can be attributed to monomeric pyrene and excimer emission, respectively. [31,32] When water content is up to 95%, the emission lifetime of **PyStBu** increased to 24.16 ns (73.81%) that is much longer than that in THF. In addition, the UV–vis absorption spectra of **PyStBu** in THF/water mixtures with 90% water content was investigated. As shown in Figure S6, the end of the absorption curve leaves off the baseline, such curve tailing phenomenon resulted in Mie scattering confirms the existence of

aggregates in the solution.[33,34] Therefore, the longer lifetime (24.16 ns) should be attributed to the aggregates.

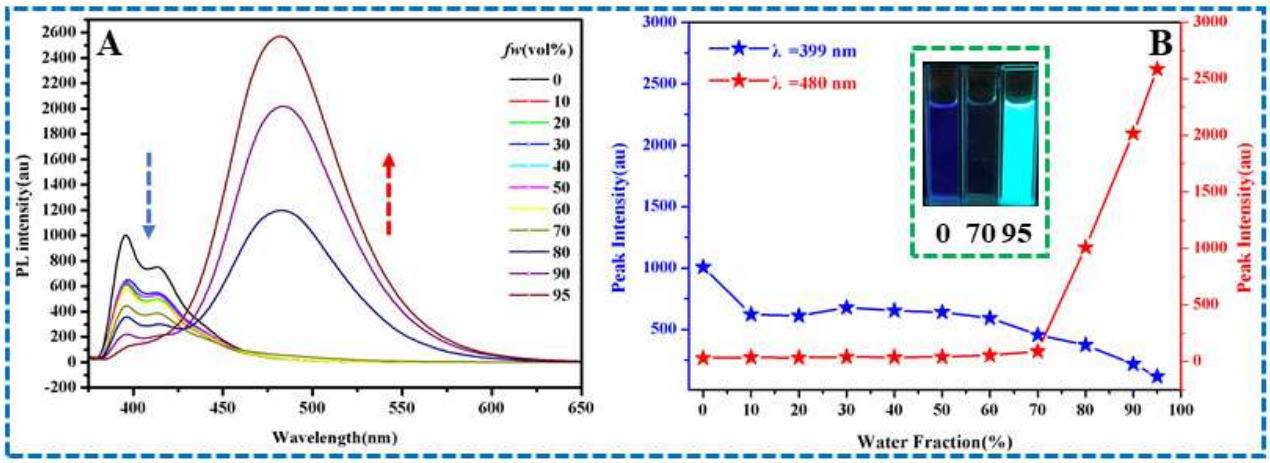

Figure 7 (A) PL spectra of **PyStBu** in THF/water mixtures with different water content. (B) Changes of PL peak intensity (399 nm and 480 nm) with water content, the data are extracted from (A). Insets of (B): Emission images of **PyStBu** in THF/water mixtures with 0, 70 and 95% water fractions. For PL measurement, concentration: the concentration of **PyStBu** in all samples used in the process of AIEE measurement are 10^{-5} M, excitation wavelength: 365 nm. Images are taken under 365 nm UV light.

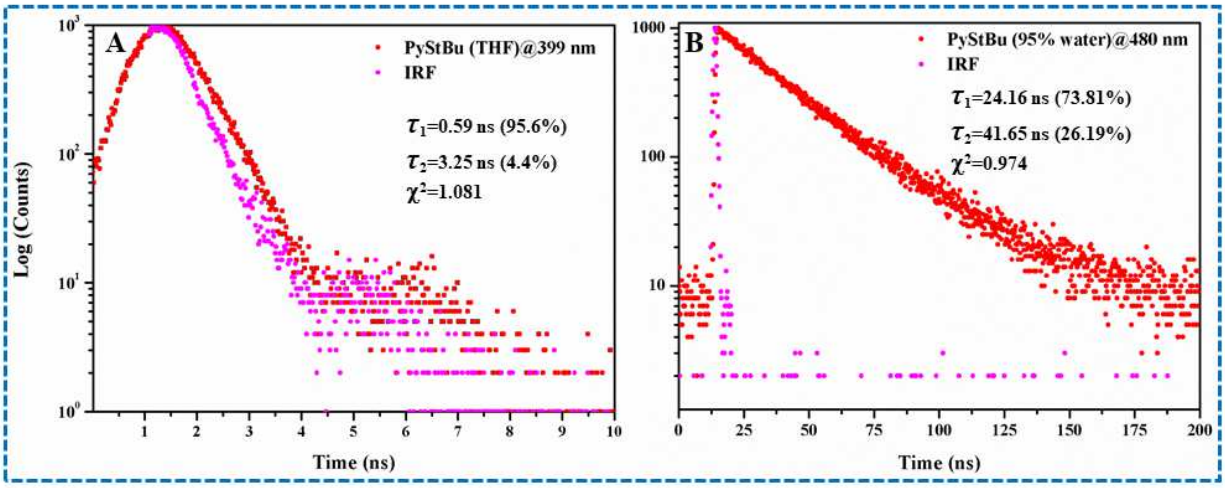

Figure 8 Time resolved fluorescence spectra of compound **PyStBu** in THF (A) and THF/H_2O (v/v =

5:95), respectively. **PyStBu** concentration: 10^{-5} M.

4 Conclusions

In conclusion, a new pyrene-based sulphide (**PyStBu**) was designed and synthesized with high yields, which exhibited successive solid-state emission changes and AIEE property. XRD, DSC and single-crystal X-ray diffraction analysis revealed that these emission changes were dominated by changes of crystal packing, intermolecular interactions or heat-induced crystal surface layer. The structure-property relationships before and after SCSC transformation were successfully illuminated in this work, which will provide reference for design and better understanding the structure-property relationships of organic solid-state luminescence materials.

Conflicts of interest

There are no conflicts to declare.

Acknowledgements

This work was supported by the Future Scientists Program of “Double First Class” of China University of Mining and Technology (2019WLKXJ013). Our deepest gratitude goes to the anonymous reviewers for their careful work and thoughtful suggestions that have helped improve this paper substantially

Notes and references

1 Takahashi S.; Miura H.; Kasai H.; Okada S.; Oikawa H.; Nakanishi H. *J. Am. Chem. Soc.* 2002, **124**, 10944-10945.

Journal Pre-proof

Journal Pre-proof

2 Chi, Z.; Zhang, X.; Xu, B.; Zhou, X.; Ma, C.; Zhang, Y.; Liu, S.; Xu, *J. Chem. Soc. Rev.* 2012, **41**, 3878−3896.

3 Yoon S. J.; Park S. Y. *J. Mater. Chem*. 2011, **21**, 8338-8346.

4 Zhao Y. F.; Gao H. Z.; Fan Y.; Zhou T. L.; Su Z. M.; Liu Y.; Wang Y. *Adv. Mater*. 2009, **21**, 3165-3169.

5 Zhang P.; Dou W.; Ju Z. H.; Tang X. L.; Liu Wei.; Chen C. Y.; Wang B.; Liu W. S. *Adv. Mater*. 2013, **25**, 6112-6116.

6 Yuan M. S.; Wang D. E.; Xue P. C.; Wang W. J.; Wang J. C.; Qin T.; Liu Z. Q.; Liu Y.; Zhang Y. R.; Wang J. Y. *Chem. Mater*. 2014, **26**, 2467-2477.

7 Mutai T.; Satou H.; Araki K. *Nat. Mater*. 2005, **4**, 658-687.

8 Abe Y.; Savikhin V.; Yin J.; Grimsdale A. C.; Soci C.; Toney M. F.; Lam Y. M. *Chem. Mater*. 2017, **29**, 7686-7696.

9 Zhang G. Q.; Lu J. W.; Sabat M.; Fraser C. L. *J. Am. Chem. Soc*. 2010, **132**, 2160-2162.

10 Choudhury A. R.; Islam K.; Kirchner M. T.; Mehta G. Row T. N. G. *J. Am. Chem. Soc*. 2004, **126**, 12274-12275.

11 Chung, H.; Diao Y. *J. Mater. Chem. C.* 2016, **4**, 3915-3933.

12 Zhang Z.; Zhang Y.; Yao D.; Bi H.; Javed I.; Fan Y.; Zhang H.; Wang Y. *Cryst. Growth Des.* 2009, **9**, 5069-5076.

13 Wang K.; Zhang H. Y.; Chen S. Y.; Yang G. H.; Zhang J. B.; Tian W. J.; Su Z. M.; Wang Y. *Adv. Mater*. 2014, **26**, 6168-6173.

14 Sun J.; Dai F. N.; Yuan W. B.; Bi W. H.; Zhao X. L.; Sun W. M.; Sun D. F. *Angew. Chem. Int. Ed.* 2011, **50**, 7061-7064.

Journal Pre-proof

15 Liu D. H.; Liu T. F.; Chen Y. P.; Zou L. F.; Feng D. W.; Wang K. C.; Zhang Q.; Yuan S.; Zhong C. L.; Zhou H. C. *J. Am. Chem. Soc.* 2005, **137**, 7740-7746.

16 Kole G. K.; Vittal J. J. Chem. Soc. Rev. 2013, 42, 1755-1775.

17 Sun H.; Sun W. H.; Jiang Y.; Wei J. H.; Zhao Y.; Zhang R.; Ni Z. H. *Dyes Pigment.* 2020, **173**, 107938.

18 Dou C. D.; Chen D.; Iqbal J.; Yuan Y.; Zhang H. Y.; Wang Y. *Langmuir* 2011, **27**, 6323-6329

19 Xu B.; Chi Z.; Zhang X.; Li H.; Chen C.; Liu S.; Zhang Y.; Xu J. *Chem. Commun*. 2011, **47**, 11080-11082.

20 Zhang Z.; Yao D.; Zhou T.; Zhang H.; Wang Y. *Chem. Commun.* 2011, **47**, 7782-7784.

21 Xu B.; Chi Z.; Zhang J.; Zhang X.; Li H.; Li X.; Liu S.; Zhang Y.; Xu J. *Chem.–Asian J.*, 2011, **6**, 1470-1478.

22 Zhang X.; Chi Z.; Zhang J.; Li H.; Xu B.; Li X.; Liu S.; Zhang Y.; Xu J. *J. Phys. Chem. B* 2011, **115**, 7606-7611.

23 Zhou X.; Li H.; Chi Z.; Zhang X.; Zhang J.; Xu B.; Zhang Y.; Liu S.; Xu J. *New J. Chem.* 2012, **36**, 685-693.

24 Li Y. F.; Xie X.; Gong X. J.; Liu M. L.; Chen R. F.; Gao D. Q. *Dyes Pigment.*, **2017**, 145: 43-53.

25 Wu H. W.; Chi W. J.; Baryshnikov G.; Wu B.; Gong Y. F.; Zheng D. X.; Xin Li, Zhao Y. L.; Liu X. G.; Åcgren H.; Zhu L. L. *Angew. Chem. Int. Ed.* 2019, **58**, 4328-4333.

26 Maji T. K.; Mostafa G.; Matsuda R.; Kitagawa S. *J. Am. Chem. Soc*. 2005, **127**, 17152-17153.

Journal Pre-proof

27 Zhao C. P.; Wang Z. L.; Yang Y. L.; Feng C.; Li W.; Li Y. A.; Zhang Y. P.; Bao F.; Xing Y. L.; Zhang X. J.; Zhang X. H. *Cryst. Growth Des.* 2012, **12**, 1227-1231.

28 Yoon S. J.; Varghese S.; Park S. K.; Wannemacher R.; Gierschner J.; Park S. Y. *Adv. Optical Mater.* 2013, **1**, 232-237.

29 Xie Z. L.; Yu T.; Chen J. R.; Ubba E.; Wang L.; Mao Z.; Su T. T.; Zhang Y.; Aldred M. P.; Chi Z. G. *Chem. Sci.* 2018, **9**, 5787-5794.

30 Xu Z. Z.; Zhang Z. W.; Jin X.; Liao Q.; Fu H. B. *Chem.–Asian J.* 2017, **12**, 2985-2990.

31 Shyamal M.; Maity S.; Mazumdar P.; Sahoo G. P.; Maity R.; Misra A. *J. Photochem. Photobiol. A: Chemistry* 2017, **342**, 1-14.

32 Li J.; Yang C.; Huang C.; Wan Y.; Lai W. Y. *Tetrahedron Lett.* 2016, **57**, 1256-1260.

33 Rakesh C.; Paramjit K.; Kamaljit S. *Anal. Chim. ACTA.* 2015, **864**, 55-63.

34 Cao Y.; Yang M.; Wang Y.; Zhou H.; Zheng J.; Zhang X.; Wu J.; Tian Y.; Wu Z. *J. Mater. Chem. C*. 2014, **2**, 3686–94.

Journal Pre-proof

Journal Pre-proof

Highlights

1. A new organic compound **PyStBu** was synthesized in high yields.
2. **PyStBu** exhibits successional solid-state emission changes induced by heating and DCM vapours fuming.
3. **PyStBu** exhibits aggregation-induced emission enhancement (AIEE) property with interesting “on–off–on” optical switching behaviour.

Journal Pre-proof

Journal Pre-proof

Conflict of Interest

The authors declared that they have no conflicts of interest to this work.

Journal Pre-proof